SUPPLEMENTARY INFORMATION

Computational modeling of pancreatic cancer reveals kinetics of metastasis suggesting optimum treatment strategies

Hiroshi Haeno[1*], Mithat Gonen[2*], Meghan B. Davis[3],
Joseph M. Herman[3,4], Christine A. Iacobuzio-Donahue[3,5+], and Franziska Michor[1+]

[1]Department of Biostatistics and Computational Biology, Dana-Farber Cancer Institute, and Department of Biostatistics, Harvard School of Public Health, Boston, MA 02115. [2]Department of Biostatistics and Epidemiology, Memorial Sloan-Kettering Cancer Center, New York, NY 10065. [3]The Sol Goldman Pancreatic Cancer Research Center, The Johns Hopkins Hospital, Baltimore, MD 21231. [4]Department of Radiation Oncology and Molecular Radiation Sciences, The Johns Hopkins Hospital, Baltimore, MD 21231. [5]Departments of Pathology, Oncology and Surgery, The Johns Hopkins Hospital, Baltimore, MD 21231. [*]These authors contributed equally to this work. [+]Authors for correspondence. Rapid autopsy, ciacobu@jhmi.edu; Mathematical modeling, michor@jimmy.harvard.edu.

TABLE OF CONTENTS

STATISTICAL ANALYSES

Although analysis of survival times is a central focus of this paper, we were not forced to use traditional survival analysis techniques, such as Kaplan-Meier estimates or proportional hazards regression, since every patient in our autopsy patient series was dead and we had complete information on survival times. For this reason, we explored more flexible and robust methods. Graphical examination of survival times suggested a lack of symmetry (the histogram of survival times had a long right tail), which can be detrimental if ignored in a classical least square analysis. We found that log-transformation sufficiently improved symmetry; for this reason, all regression analyses correlating survival with tumor and treatment-related variables were performed using multiplicative (exponential) regression. To improve the robustness of our conclusions, we looked for potentially influential outlying observations and found two such points using the PRESS statistics; therefore, we estimated the model parameters using robust exponential regression instead of least squares (Table S2c). In particular, we used the M-method of Huber (Huber, 1973) with a bi-square weight function and the median method to estimate the scale parameter. The advantages of this method over least squares is that it gives higher weights to data points closer to the center and less weights to those in the tails, minimizing the influence of outliers. No leverage points were identified. The model fit was assessed by R^2, Akaike's information criterion (AIC), distribution of the standardized residuals, and by plotting predicted survival against the observed.

The coefficients in Table S2c are on a multiplicative scale; for example, surgical removal of the primary almost doubles predicted survival ($e^{0.632}$=1.88) when growth rates and size of the largest metastatic tumor at diagnosis were held constant. One unit increase in either the primary or the metastatic growth rate (other factors kept constant) decreased predicted survival by approximately 22%, and one cm increase in the largest metastatic tumor decreased predicted survival by 32%. All of these factors were significantly associated with survival. This robust regression model had a good fit (R^2 = 0.41, AIC=102.9) and approximately normally distributed residuals (Figure S1).

ACQUISITION OF METASTATIC ABILITY BY TWO ALTERATIONS

We initially assumed that tumor cells acquire the ability to disseminate and metastasize by acquiring a single (epi)genetic alteration (see main text for discussion of the model and results). We then extended our mathematical framework to include the scenario in which two (epi)genetic alterations are necessary to confer metastatic ability to tumor cells. We investigated two cases for this scenario: (i) two (epi)genetic alterations arise in a metastasis suppressor gene in a genetically stable cell; in this case, the mutation rate altering the first allele of the metastasis suppressor is the same order of magnitude as that in the model presented in the main text, while the mutation rate altering the second allele of the metastasis suppressor is half that the first mutation rate since there is only one allele left that can be mutated; and (ii) an (epi)genetic alteration occurs in a metastasis suppressor gene followed by a loss of heterozygosity (LOH) event inactivating the second allele in a genetically unstable cell; in this case, the mutation rate inactivating the second allele is much larger than the first mutation rate. Furthermore, we used the mathematical model to investigate the effects of the assumption of two necessary mutations for the metastatic phenotype on the metastatic profile of patients. In order to compare the results of this model to the one presented in the main text, we fixed the product of the two mutation rates to the value used for the single mutation rate in the model presented in the main text.

The mathematical framework

We designed a mathematical model of pancreatic cancer growth and dissemination to investigate the dynamics of cancer cells, the survival of patients, and optimum intervention strategies. The model considers exponential expansion of pancreatic cancer cells starting from a single cell that has not yet evolved the ability to metastasize. We chose an exponential model over other functional forms since the exponential model provided a better fit to the data as compared to a linear model (see main text) and does not require as many data points to be reliably fit as some of the more complex models. In the context of our mathematical model, the cells follow a stochastic process: during each elementary time step, a cell is chosen proportional to fitness for reproduction, death, or export from the primary tumor to establish a metastatic colony elsewhere. Time is measured in numbers of cell divisions. Cells that have not yet acquired the

ability to metastasize are called type-s0 cells. These cells divide at rate r and die at rate d per time unit. The first alteration towards the metastatic phenotype occurs with probability v_1 per cell division. Cells carrying this alteration are called type-s1 cells. They divide at rate s_1 and die at rate d_1 per time unit. Once a type-s1 cell has arisen, the second alteration towards the metastatic phenotype arises with probability v_2 in such a cell. The probability of acquiring both alterations during a single cell division is sufficiently small to be neglected in our framework. Cells carrying two (epi)genetic alterations are called type-s2 cells. They divide at rate s_2, die at rate d_2, and may be exported from the primary tumor to attempt the establishment of metastases elsewhere. The integrated rate of leaving the primary site and founding a new colony at a distant site is denoted by q. Once disseminated, the cells are called type-s3 cells and proliferate and die with rates s_3 and d_3, respectively.

The total number of tumor cells (including all four types) at diagnosis is denoted by M_1, and the total number of tumor cells at autopsy is given by M_2. Here diagnosis refers to the initial detection of the tumor when the patient is first admitted to the hospital, and autopsy refers to the time of patient death when the tumor burden is assessed and the cause of death is determined. We expect that all four cell types contribute to the size at diagnosis since in rare cases, metastatic disease with unknown primary is diagnosed, where only type-s3 cells can be detected. Once the tumor has been diagnosed with a population size of M_1, there are four options: (i) there may be no treatment due to the advanced age of the patient or other complications; (ii) the patient may receive surgery, which removes a fraction ε of the primary tumor; (iii) the patient may undergo chemotherapy, which reduces the growth rate of all cells by a factor of γ; or (iv) the patient may receive surgery and chemotherapy.

Computer simulations

We performed exact computer simulations of the stochastic process. There are four types of cells: type-s0, type-s1, type-s2 and type-s3 cells. Their respective numbers are denoted by x, y_1, y_2 and z_i; the latter specifies the number of cells in the i-th metastatic site. A change in x, y_1, y_2 and z_i can occur by cell division (possibly with mutation), cell death, or export from the primary site. Each time an export event occurs, a new metastatic colony is established. The total number of sites where tumor cells can found

metastases is denoted by I. Initially, there is one type-s0 cell, x =1, and no type-s1, type-s2, or type-s3 cells, $y_1 = y_2 = z_i = 0$ for all $i \in I$.

The stochastic simulation is performed by determining the probabilities of all possible events – the production and death of a type-s0, -s1, -s2 or –s3 cell and the export of a type-s2 cell to found a new metastatic site. The chance of each event occurring is proportional to its rate normalized by the sum of the rates of all possible events, given by $\Gamma = (r+d)x + (s_1+d_1)y_1 + (s_2+d_2+q)y_2 + \sum_{i=1}^{I}(s_3+d_3)z_i$. The timing of the first event is given by a negative exponential distribution with mean $1/\Gamma$. The process is continued either until all cells go extinct, $x = y_1 = y_2 = \sum_i z_i = 0$, or until the total cell number reaches the final size, $x + y_1 + y_2 + \sum_i z_i = M_1$ at diagnosis or $x + y_1 + y_2 + \sum_i z_i = M_2$ at autopsy.

The transition probabilities between states of the stochastic process are determined as follows. The number of type-s0 cells increases if a type-s0 cell divides without mutating. Hence the probability that the number of type-s0 cells increases by one is given by

$$\Pr[(x,y_1,y_2,z_1,...,z_I) \to (x+1,y_1,y_2,z_1,...,z_I)] = xr(1-v_1)/\Gamma. \qquad \text{(S1a)}$$

The number of type-s1 cells increases by mutation of a type-s0 cell or by division of a type-s1 cell. The probability that the number of type-s1 cells increases by one is given by

$$\Pr[(x,y_1,y_2,z_1,...,z_I) \to (x,y_1+1,y_2,z_1,...,z_I)] = (xrv_1 + y_1s_1(1-v_2))/\Gamma. \qquad \text{(S1b)}$$

The number of type-s2 cells increases by mutation of a type-s1 cell or by division of a type-s2 cell. The probability that the number of type-s2 cells increases by one is given by

$$\Pr[(x,y_1,y_2,z_1,...,z_I) \to (x,y_1,y_2+1,z_1,...,z_I)] = (y_1s_1v_2 + y_2s_2)/\Gamma. \qquad \text{(S1c)}$$

Export of a type-s2 cell to a new metastatic site ($j \in I$) increases the number of metastatic sites by one and decreases the number of type-s3 cells by one,

$$\Pr[(x,y_1,y_2,z_1,...,z_j=0,...,z_I) \to (x,y_1,y_2-1,z_1,...,z_j=1,...,z_I)] = y_2 q/\Gamma . \quad \text{(S1d)}$$

The probability that the number of type-s3 cells increases by one in the *i*-th metastatic site is given by

$$\Pr[(x,y_1,y_2,z_1,...,z_i,...,z_I) \to (x,y_1,y_2,z_1,...,z_i+1,...,z_I)] = z_i s_3/\Gamma . \quad \text{(S1e)}$$

The probabilities that the numbers of type-s0, type-s1, type-s2, and type-s3 cells decrease by one are given by

$$\begin{aligned}
&\Pr[(x,y_1,y_2,z_1,...,z_I) \to (x-1,y_1,y_2,z_1,...,z_I)] = xd/\Gamma \\
&\Pr[(x,y_1,y_2,z_1,...,z_I) \to (x,y_1-1,y_2,z_1,...,z_I)] = y_1 d_1/\Gamma \\
&\Pr[(x,y_1,y_2,z_1,...,z_I) \to (x,y_1,y_2-1,z_1,...,z_I)] = y_2 d_2/\Gamma \\
&\Pr[(x,y_1,y_2,z_1,...,z_i,...,z_I) \to (x,y_1,y_2,z_1,...,z_i-1,...,z_I)] = z_i d_3/\Gamma
\end{aligned} . \quad \text{(S1f)}$$

For each parameter set, we performed many independent runs of the stochastic process to account for random fluctuations, and counted the fraction of runs that reach the final size, M_1 or M_2, and have produced at least one type-s3 cell. We also recorded the number of metastatic sites with non-zero cell numbers, the total number of type-s3 cells in those sites, and the time between diagnosis and autopsy.

Results

We then investigated the effects of four treatment options utilizing this new model. We considered the division rates of primary tumor cells to be the same no matter whether they harbor no, one or two mutations, $r = s_1 = s_2$, and similarly considered the death rates of all tumor cells to be the same, $d = d_1 = d_2 = d_3$. Figure S2a-j displays the dependence of the survival time of patients after diagnosis on the parameters of the mathematical framework. In this analysis, we comprehensively investigated a wide region of each parameter instead of using the values we estimated in the main text since

those estimates were obtained using the original version of the framework. We found that our conclusions presented in the main text remain robust, as a reduction of the growth rate is more effective for prolonging survival than resection of the primary tumor by surgery (Fig. S2). Comparing the cases in which the second mutation rate represents genetically stable and unstable cells, respectively, we found that the treatment effect on survival is mostly unchanged except when the death rate, mutation rate, and metastatic rate are all large (Fig. S2b, d, e, g, i, and j). In those parameter regions, metastatic cells are more likely to exist in the case of genetically unstable cells, and treatment dose not prolong survival to a large extent.

A reduction of growth rates by the administration of chemotherapy effectively prolongs survival when the growth rate of primary tumor cells is small (Fig. S2a and f). When the growth rate is close to the death rate, then the net growth rate effectively decreases once the growth rate is reduced. When the death rate of tumor cells is sufficiently large, then a large reduction of the growth rate decreases the net growth rate to a negative value and in such cases, the number of cancer cells became zero (data not shown). However, in situations in which the drug effect is low enough so that the net growth rate of tumor cells remains positive, or in situations in which the tumor is resected, survival times increase compared to cases without treatment (Fig. S2b and g). In cases when the death rate and the second mutation rate are large, metastatic cells are more likely to exist at the time of diagnosis as compared to cases with small second mutation rates. If the net growth rate of metastatic cells is larger than that of primary cells, the survival time after drug treatment decreases and resection of the primary tumor is not effective (Fig. S2g); however, when the number of tumor cells at diagnosis is large, resection is effective (Fig. S2c and h). Also, the survival time with large second mutation rates does not depend on the mutation rate and metastatic rate (Fig. S2d and e), but treatment is not effective when the mutation rate and metastatic rate are large because of the existence of metastatic cells (Fig. S2i and j).

Moreover, we investigated the dependence of three quantities on the system parameters: the probability of metastasis, the expected number of metastatic sites, and the expected number of metastatic cells when the number of tumor cells reaches a certain size such as the tumor size at diagnosis and autopsy. We found that the probability of metastasis

decreases with an increasing growth rate of primary cells because a quickly growing tumor has a low chance of accumulating mutations and acquiring the ability to metastasize before reaching a certain size (Fig S3a). As the death rate and the number of tumor cells at autopsy increase, the probability of metastasis also increases (Fig. S4a and S5a). An increase of the mutation rate and of the metastatic rate increases the probability of metastasis (Fig. S6a and d). Figures S7a and d show the probability of metastasis at autopsy when the primary tumor is resected at diagnosis or chemotherapy is initiated at diagnosis. Interestingly, both treatment options increase the probability of metastasis since they prolong the survival time (i.e. time until autopsy); this delay leads to an increase in the eventual probability of metastasis. When the second mutation rate is large, then the probability of metastasis increases (Fig. S3-S7d); the dependence on each parameter, however, does not change in that case.

Next we investigated the parameter dependence of the expected number of metastatic sites conditional to metastatic cells being present when the second mutation rate is low (Fig. S3-S7b, S6e, and S7e). The growth rate of primary tumor cells does not affect the expected number of metastatic sites to a large extent and the expected number of metastatic cells is low (Fig. S3b); this finding implies that there are few chances of dissemination in this parameter region. When the death rate is large, the expected number of metastatic sites is large (Fig. S4b) since a large death rate reduces the net growth rate close to zero. This process in turn leads to a larger risk of dissemination. When the number of tumor cells at autopsy and the mutation rate are large, then the expected number of metastatic sites is also large (Fig. S5b and S6b). We found that an optimal metastatic rate exists such that the number of metastatic sites is maximized (Fig. S6e). This optimum exists due to a delicate balance: when the metastatic rate is large, then there are many chances of dissemination; however, when the metastatic rate becomes too large as compared to mutation rates, then metastatic sites arise from only a few type-s2 cells that have acquired the potential to metastasize. In that case, metastatic growth at a few sites is likely to be dominant and those colonies will increase in number before other cells disseminate from the primary tumor. Treatment options increase the expected number of metastatic sites (Fig. S7b and e) by slowing down the expansion of both primary and metastatic tumors.

In cases in which the second mutation for acquiring metastatic ability occurs frequently, the dependence on several parameters such as growth rate of primary tumor, death rate, and metastatic rate differs from cases with small second mutation rates (Fig. S3-S7e, S6b, and S7b). For instance, when the growth rate of primary tumor cells is low, the primary tumor grows slowly and the chance of dissemination increases (Fig. S3e). This effect appears when the number of the cells that have acquired potential to metastasize is large because of the large second mutation rates. However, when the death rate is too large, the number of metastatic sites is small (Fig. S4e). Once a metastatic site has arisen, metastatic cells with a larger growth rate as compared to primary tumor cells have an enhanced chance to increase in number and become dominant, which in turn decreases the risk of dissemination from a primary tumor. When both metastatic rate and mutation rate are large, then, as expected, expected number of metastatic sites increases (Fig. S6e). Furthermore, the parameter dependence of the number of metastatic cells conditional to metastases having emerged is shown in Fig. S3c, S4c, S5c, S6c, S6f, S7c and S7f. Here, the dependence is very similar to that of probability of metastasis. Especially when the treatment effect is large, the number of metastatic cells increases quickly because treatment slows down tumor growth and results in an increase in the emergence and growth of metastatic cells (Fig. S7c and f).

Lastly, we investigated how the metastatic profiles vary between the original model (one alteration necessary for the metastatic phenotype) and the new model (two alterations necessary for the metastatic phenotype). We considered the product of the two mutation rates in the new model to be the same as the mutation rate of the original model and compared the probability of metastasis, the expected number of metastatic sites, and the expected number of metastatic cells (Fig. S3g-i, S4g-i, S5g-i, S6a-f, and S7a-f). The probability and the expected number of metastatic sites increases in the new model. The number of cancer cells with metastatic ability (type-1 cells or type-s2 cells) at a certain size of the primary tumor is a good quantity for comparing the two models. The number of type-1 cells at time t, where one type-0 cell starts clonal expansion at time 0, is deterministically approximated by $\int_0^t rue^{(r-d)x}e^{(a_1-b_1)(t-x)}dx$. When we assume a homogeneous population of primary tumor cells with respect to the growth and death rates, the number of type-1 cells at time t is given by

$$\int_0^t rue^{(r-d)t}dx = rute^{(r-d)t}, \tag{S2}$$

while the number of type-s2 cells at time t is approximately given by

$$\begin{aligned}&\int_0^t\int_0^{x_2} rv_1e^{(r-d)x_1}e^{(s_1-d_1)(x_2-x_1)}dx_1s_1v_2e^{(s_2-d_2)(t-x_2)}dx_2\\&= \int_0^t rs_1v_1v_2x_2e^{(r-d)t}dx_2 = r^2v_1v_2t^2e^{(r-d)t}/2\end{aligned}. \tag{S3}$$

Since the product of two mutation rates in the new model is considered to be the same as the mutation rate of the original model ($u = v_1v_2$), the ratio of the number of type-s2 cells at time t to that of type-1 cells is given by $rt/2$. Assuming deterministic growth of primary tumor cells and ignoring the metastatic population, the ratio at diagnosis becomes $\frac{\log(M_1)}{2(1-d/r)}$. When $r > d$ and $M_1 >> 1$, then the number of type-s2 cells is larger than that of type-1 cells. This fact leads to a large probability of metastasis and a large number of metastatic sites in the new model (Fig. S3g-h, S4g-h, S5g-h, S6a-b, S6d-e, S7a-b, and S7d-e). There is an optimum value of the death rate, which maximizes the expected number of metastatic sites in Fig. S4h, because slow net expansion of primary tumor cells due to an increasing death rate increases the chance of dissemination. However, an excessively large death rate renders metastatic cells with a larger growth rate dominant, which in turn decreases the risk of dissemination from the primary tumor.

The number of metastatic cells conditional to metastatic cells being present does not change to a large extent between two models with regard to variation of the growth and mutation rates (Fig. S3i and S6c). The number of metastatic cells is larger in the original model than that in the new model when testing different death rates (Fig. S4i). We also found that when the number of tumor cells at autopsy and the metastatic rate are large, more metastatic cells exist in the new model as compared to the original model (Fig S5i and S6f). Finally, both resection and drug administration increase the number of metastatic cells in the new model as compared to the original model (Fig. S7c and f).

Conclusions

In summary, we have investigated the effects of the assumption in which the metastatic ability of tumor cells is acquired by two (epi)genetic alterations rather than a single mutation. We found that the qualitative effect of administration of chemotherapy to prolong survival does not change by addition of this assumption to the framework (Fig. S2). We also showed the dependence of the probability of metastasis, the expected number of metastatic sites, and the expected number of metastatic cells on all parameters in the new model (Fig. S3-S7). Finally, we found that if we fix the product of the mutation rates to be the same as the mutation rate in the original model, then the probability of metastasis, the expected number of metastatic sites and the expected number of metastatic cells within patients who receive resection and drug administration increase in the new as compared to the original model (Fig. S3-S7).

SUPPLEMENTARY REFERENCES

Huber, P.J. (1973). Robust regression: Asymptotics, conjectures and monte carlo. Ann Statist *1*, 799-821.

SUPPLEMENTARY FIGURE LEGENDS

Figure S1. Statistical analysis of the pancreatic cancer patient dataset containing 101 patients. (a) Correlations between growth rates of primary and metastatic tumors and log-survival time. Primary tumors are shown in black while metastatic tumors are shown in white. (b) Distribution of the standardized residuals from the multiplicative robust regression model of survival times and the factors listed in Table S2c. There is no evidence of poor fit based on this residual plot. (c) Q-Q plot for the residuals. The horizontal axis represents the quantile from the normal distribution and the vertical axis the quantile of the standardized residual. With most points on or near the line of equality, this figure indicates no serious departures from the presumed regression model.

Figure S2. Survival after treatment. The figure shows the effect of several treatment options on the survival of patients, in dependence of different parameter values. Panels a, b, c, d, and e show the case in which the second mutation rate is relatively small ($v_2 = v_1/2$) and panels f, g, h, i, and j show the case in which the second mutation rate is large ($v_2 = 0.1$). The circles connected by lines indicate the results of the direct computer simulations. Black, red dotted, blue, red, and purple curves respectively represent no treatment, 50% reduction of growth rates by drug, 99% of primary tumor removed by resection, 90% reduction of growth rates by drug and both 90% reduction of growth rates and 90% primary tumor reduction after diagnosis. The parameter region where the net growth rate of primary tumor becomes negative is not shown (panel b and g). Parameter values are $M_1 = 250000$, $M_2 = 1000000$, $r = s_1 = s_2 = 0.11$, s_3=0.21, d=d_1=d_2=d_3=0.01, $v_1 = 10^{-3}$, and $q = 10^{-4}$.

Figure S3. The dependence of metastatic quantities on the grow rate of primary tumor cells. The figure shows the dependence of the three quantities, probability of metastasis, expected number of metastatic sites, and expected number of metastatic cells, on the growth rate of primary tumor cells. The circles connected by lines indicate the results of the direct computer simulations. Panels a, b, and c show the case in which the second mutation rate is relatively small ($v_2 = v_1/2$), panels d, e, and f show the case in which the second mutation rate is large ($v_2 = 0.1$), and panels g, h, and i show the case in which the product of the mutation rates in the new model is fixed as the mutation rate in the original model. Black and red curves in panels g, h, and i, indicate the results of the original model in the main text and the new model where two (epi)genetic mutations confer metastatic ability to tumor cells, respectively. Parameter values are $M_1 = 250000$, $M_2 = 1000000$, a_2=s_3=0.21, d=d_1=d_2=d_3=b_1=b_2=b_3=0.01,, $v_1 = 10^{-3}$ (a-f), $v_1 = 10^{-2}$ (g-i), $v_2 = 10^{-2}$ (g-i), $u = 10^{-4}$ (g-i), $q = 10^{-4}$, $\varepsilon = 0$, and $\gamma = 0$.

Figure S4. The dependence of metastatic quantities on the death rate. The figure shows the dependence of the three quantities, probability of metastasis, expected number of metastatic sites, and expected number of metastatic cells, on the death rate. The circles connected by lines indicate the results of the direct computer simulations. Panels a, b, and c show the case in which the second mutation rate is relatively small

($v_2 = v_1/2$), panels d, e, and f show the case in which the second mutation rate is large ($v_2 = 0.1$), and panels g, h, and i show the case in which the product of the mutation rates in the new model is fixed as the mutation rate in the original model. Black and red curves in panels g, h, and i, indicate the results of the original model in the main text and the new model where two (epi)genetic mutations confer metastatic ability to tumor cells, respectively. Parameter values are $M_1 = 250000$, $M_2 = 1000000$, $r=a_1=s_1=s_2=0.11$, $a_2=s_3=0.21$, $v_1 = 10^{-3}$ (a-f), $v_1 = 10^{-2}$ (g-i), $v_2 = 10^{-2}$ (g-i), $u = 10^{-4}$ (g-i), $q = 10^{-4}$, $\varepsilon = 0$, and $\gamma = 0$.

Figure S5. The dependence of metastatic quantities on the number of tumor cells at autopsy. The figure shows the dependence of the three quantities, probability of metastasis, expected number of metastatic sites, and expected number of metastatic cells, on the number of tumor cells at autopsy. The circles connected by lines indicate the results of the direct computer simulations. Panels a, b, and c show the case in which the second mutation rate is relatively small ($v_2 = v_1/2$), panels d, e, and f show the case in which the second mutation rate is large ($v_2 = 0.1$), and panels g, h, and i show the case in which the product of the mutation rates in the new model is fixed as the mutation rate in the original model. Black and red curves in panels g, h, and i, indicate the results of the original model in the main text and the new model where two (epi)genetic mutations confer metastatic ability to tumor cells, respectively. Parameter values are $M_1 = 250000$, $r=a_1=s_1=s_2=0.11$, $a_2=s_3=0.21$, $d=d_1=d_2=d_3=b_1=b_2=b_3=0.01$, $v_1 = 10^{-3}$ (a-f), $v_1 = 10^{-2}$ (g-i), $v_2 = 10^{-2}$ (g-i), $u = 10^{-4}$ (g-i), $q = 10^{-4}$, $\varepsilon = 0$, and $\gamma = 0$.

Figure S6. The dependence of metastatic quantities on the mutation and metastatic rates. The figure shows the dependence of the three quantities, probability of metastasis, expected number of metastatic sites, and expected number of metastatic cells, on the mutation and metastatic rates. The circles connected by lines indicate the results of the direct computer simulations. Panels a, b, and c show the dependence on the mutation rate, while panels d, e, and f show the dependence on the metastatic rate. Blue and red curves indicate the case in which the second mutation rate is relatively small

($v_2 = v_1/2$), and in which the second mutation rate is large ($v_2 = 0.1$). Black curve indicates the results of the original model in the main text, while green and yellow curves indicate the results of the new model where two (epi)genetic mutations confer metastatic ability to tumor cells. In panels a, b, and c, green curves examine different values of the first mutation rate in the new model (from $v_1 = 10^{-3}$ to $v_1 = 10^{-0.5}$) with the second mutation rate fixed as $v_2 = 10^{-2}$ and the horizontal axes in the panels are shown as the product of two mutation rates to compare the dependence on the mutation rate in the original model; yellow curves examine different values of the second mutation rate in the same way as green curves. Parameter values are $M_1 = 250000$, $M_2 = 1000000$, $r=a_1=s_1=s_2=0.11$, $a_2=s_3=0.21$, $d=d_1=d_2=d_3=b_1=b_2=b_3=0.01$, $q = 10^{-4}$ (a-c), $v_1 = 10^{-3}$ (d-f, red and blue), $v_1 = 10^{-2}$ (d-f, green and yellow), $v_2 = 10^{-2}$ (d-f, green and yellow), $u = 10^{-4}$, $\varepsilon = 0$, and $\gamma = 0$.

Figure S7. The dependence of metastatic quantities on treatment options. The figure shows the dependence of the three quantities, probability of metastasis, expected number of metastatic sites, and expected number of metastatic cells, on the resection and reduction of growth rate by chemotherapy. The circles connected by lines indicate the results of the direct computer simulations. Panels a, b, and c show the dependence on the resection effect, while panels d, e, and f show the dependence on the reduction of growth rate. Blue and red curves indicate the case in which the second mutation rate is relatively small ($v_2 = v_1/2$), and in which the second mutation rate is large ($v_2 = 0.1$). Black curve indicates the results of the original model in the main text, while green curve indicates the results of the new model where two (epi)genetic mutations confer metastatic ability to tumor cells. Parameter values are $M_1 = 250000$, $M_2 = 1000000$, $r=a_1=s_1=s_2=0.11$, $a_2=s_3=0.21$, $d=d_1=d_2=d_3=b_1=b_2=b_3=0.01$, $v_1 = 10^{-3}$ (red and blue), $v_1 = 10^{-2}$ (green), $v_2 = 10^{-2}$ (green), $u = 10^{-4}$, $q = 10^{-4}$, $\varepsilon = 0$ (d-f), and $\gamma = 0$ (a-c).

SUPPLEMENTARY TABLES

Table S1: (a) The autopsy patient cohort containing 101 patients and (b) survival indices from information at diagnosis based upon the adjuvant cohort (127 patients.

Table S2: Correlations between various measures of tumor size and growth rate as well as survival in the autopsy cohort (101 patients) when using a diameter of 0.2 cm (a) and 0.05 (b) for undetectable metastases, and (c) exponential coefficients of model parameters with respect to the survival time, based upon the autopsy cohort (101 patients).

Supplemental Figures

Click here to download Supplemental Figure: SI figures.ppt

Fig. S1

a

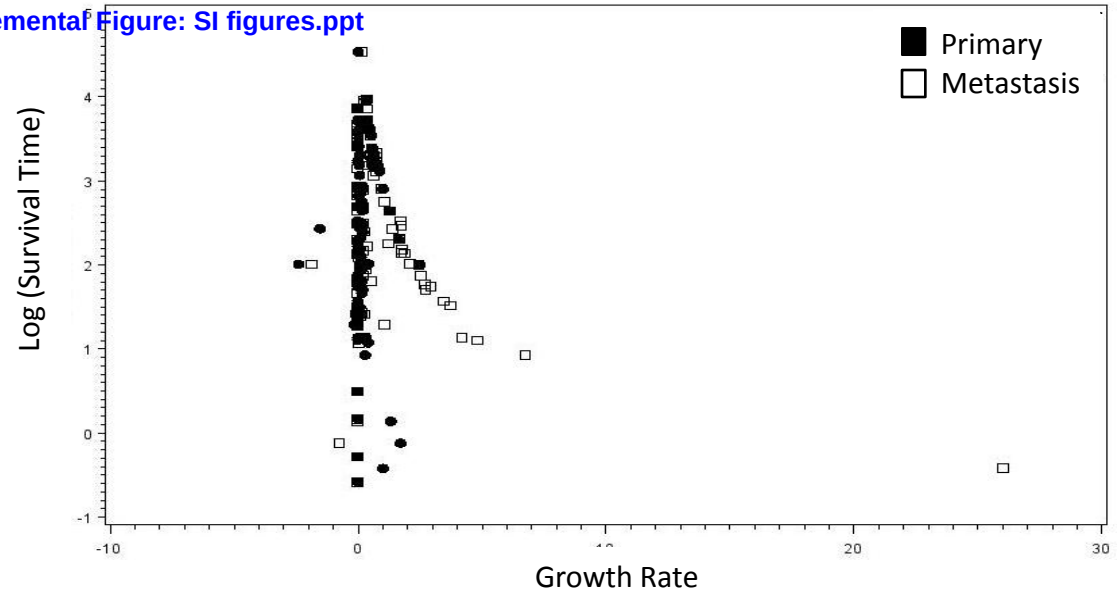

b

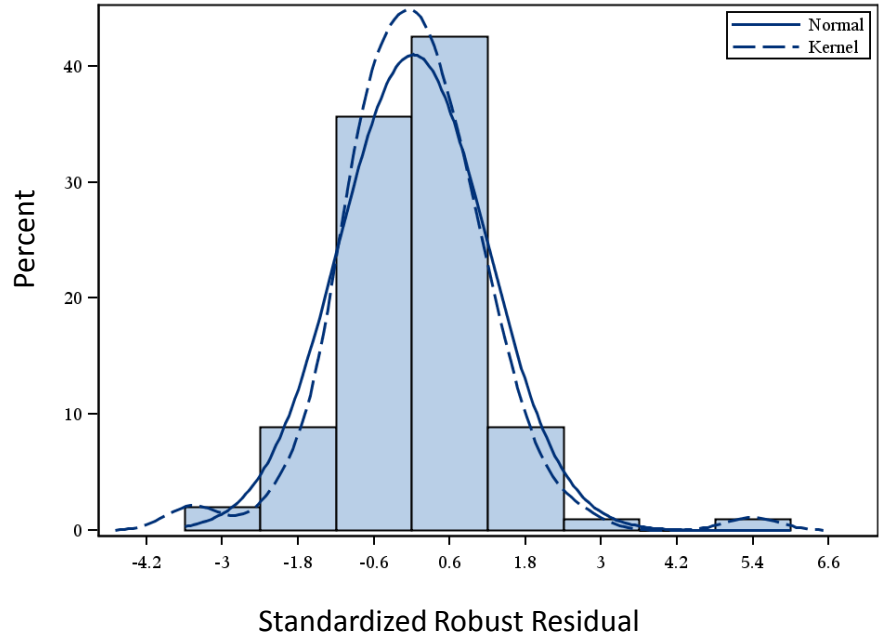

c

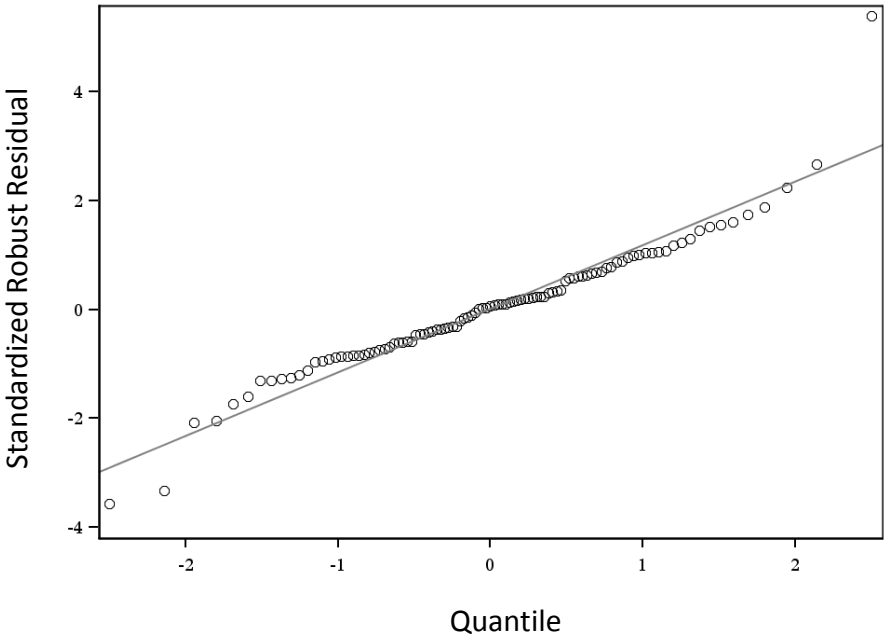

Fig. S2

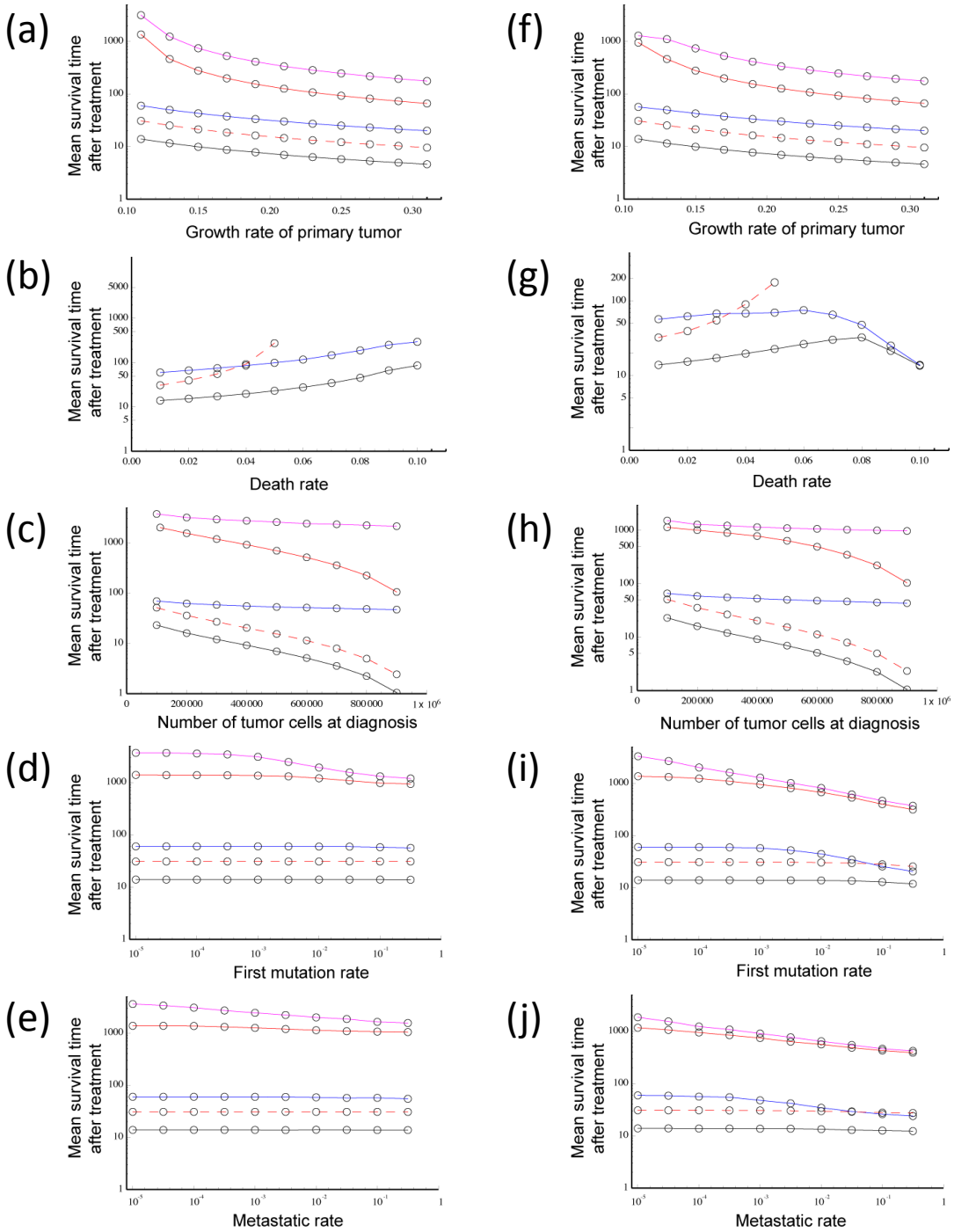
(a)
Mean survival time after treatment
Growth rate of primary tumor
(f)
Mean survival time after treatment
Growth rate of primary tumor
(b)
Mean survival time after treatment
Death rate
(g)
Mean survival time after treatment
Death rate
(c)
Mean survival time after treatment
Number of tumor cells at diagnosis
(h)
Mean survival time after treatment
Number of tumor cells at diagnosis
(d)
Mean survival time after treatment
First mutation rate
(i)
Mean survival time after treatment
First mutation rate
(e)
Mean survival time after treatment
Metastatic rate
(j)
Mean survival time after treatment
Metastatic rate

Fig. S3

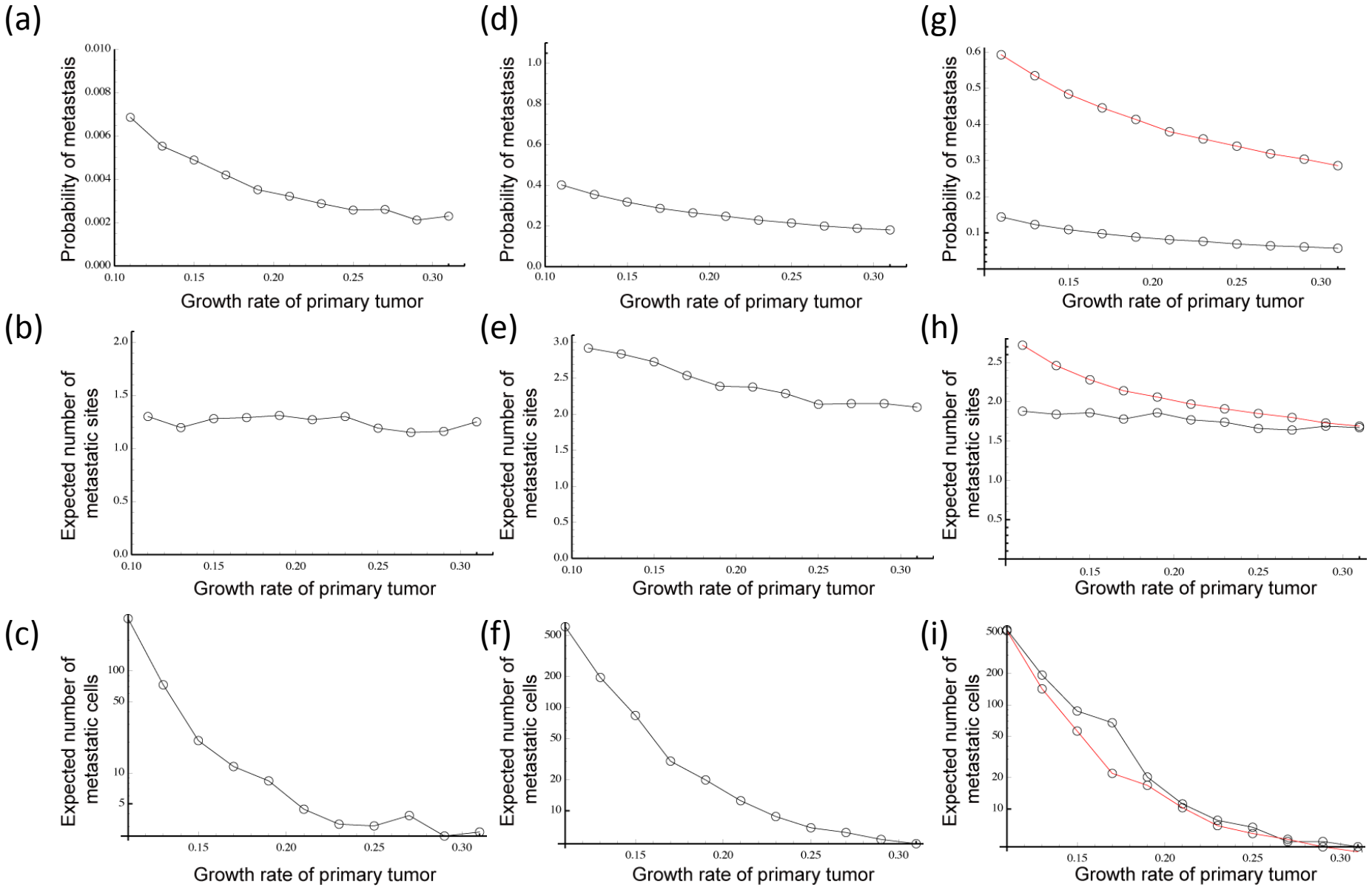
(a)
Probability of metastasis
0.010
0.008
0.006
0.004
0.002
0.000
0.10
0.15
0.20
0.25
0.30
Growth rate of primary tumor
(d)
Probability of metastasis
1.0
0.8
0.6
0.4
0.2
0.0
0.10
0.15
0.20
0.25
0.30
Growth rate of primary tumor
(g)
Probability of metastasis
0.6
0.5
0.4
0.3
0.2
0.1
0.15
0.20
0.25
0.30
Growth rate of primary tumor
(b)
Expected number of metastatic sites
2.0
1.5
1.0
0.5
0.0
0.10
0.15
0.20
0.25
0.30
Growth rate of primary tumor
(e)
Expected number of metastatic sites
3.0
2.5
2.0
1.5
1.0
0.5
0.0
0.10
0.15
0.20
0.25
0.30
Growth rate of primary tumor
(h)
Expected number of metastatic sites
2.5
2.0
1.5
1.0
0.5
0.15
0.20
0.25
0.30
Growth rate of primary tumor
(c)
Expected number of metastatic cells
100
50
10
5
0.15
0.20
0.25
0.30
Growth rate of primary tumor
(f)
Expected number of metastatic cells
500
200
100
50
20
10
0.15
0.20
0.25
0.30
Growth rate of primary tumor
(i)
Expected number of metastatic cells
500
200
100
50
20
10
0.15
0.20
0.25
0.30
Growth rate of primary tumor

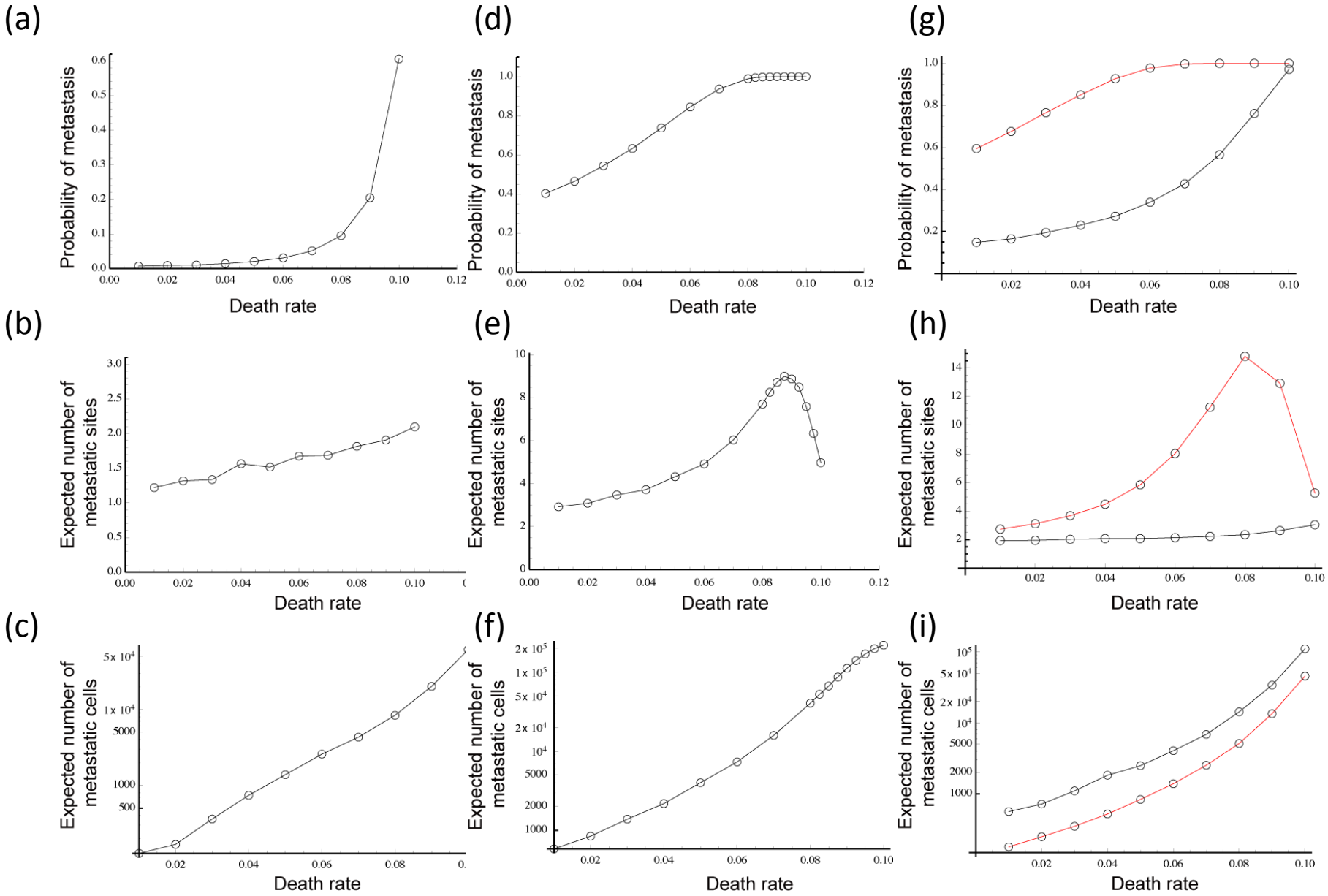
(a)
Probability of metastasis
Death rate
(d)
Probability of metastasis
Death rate
(g)
Probability of metastasis
Death rate
(b)
Expected number of metastatic sites
Death rate
(e)
Expected number of metastatic sites
Death rate
(h)
Expected number of metastatic sites
Death rate
(c)
Expected number of metastatic cells
Death rate
(f)
Expected number of metastatic cells
Death rate
(i)
Expected number of metastatic cells
Death rate

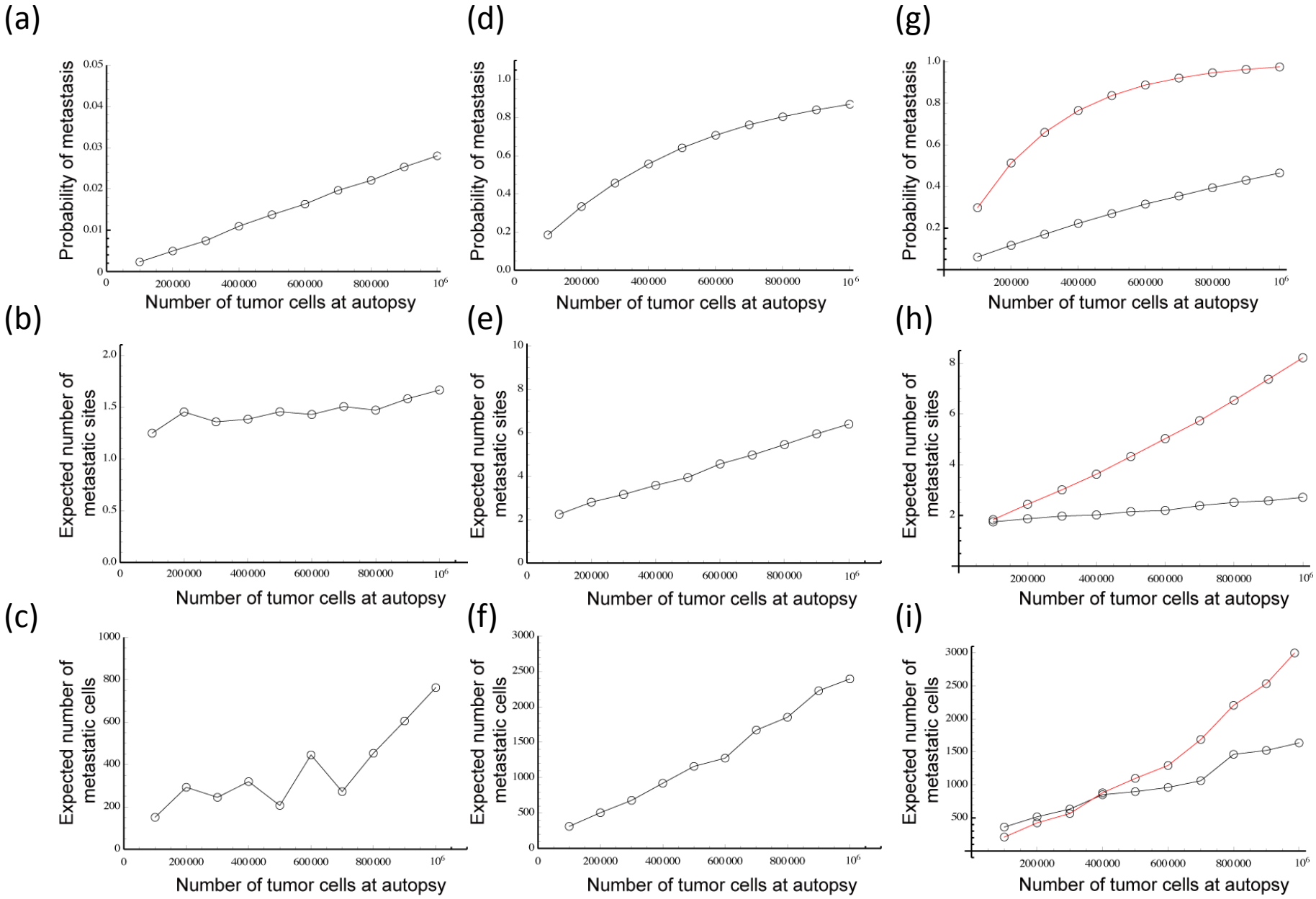
(a)
Probability of metastasis
0.05
0.04
0.03
0.02
0.01
0
200 000
400 000
600 000
800 000
10^6
Number of tumor cells at autopsy
(d)
Probability of metastasis
1.0
0.8
0.6
0.4
0.2
0.0
200 000
400 000
600 000
800 000
10^6
Number of tumor cells at autopsy
(g)
Probability of metastasis
1.0
0.8
0.6
0.4
0.2
200 000
400 000
600 000
800 000
10^6
Number of tumor cells at autopsy
(b)
Expected number of metastatic sites
2.0
1.5
1.0
0.5
0.0
200 000
400 000
600 000
800 000
10^6
Number of tumor cells at autopsy
(e)
Expected number of metastatic sites
10
8
6
4
2
0
200 000
400 000
600 000
800 000
10^6
Number of tumor cells at autopsy
(h)
Expected number of metastatic sites
8
6
4
2
200 000
400 000
600 000
800 000
10^6
Number of tumor cells at autopsy
(c)
Expected number of metastatic cells
1000
800
600
400
200
0
200 000
400 000
600 000
800 000
10^6
Number of tumor cells at autopsy
(f)
Expected number of metastatic cells
3000
2500
2000
1500
1000
500
0
200 000
400 000
600 000
800 000
10^6
Number of tumor cells at autopsy
(i)
Expected number of metastatic cells
3000
2500
2000
1500
1000
500
200 000
400 000
600 000
800 000
10^6
Number of tumor cells at autopsy

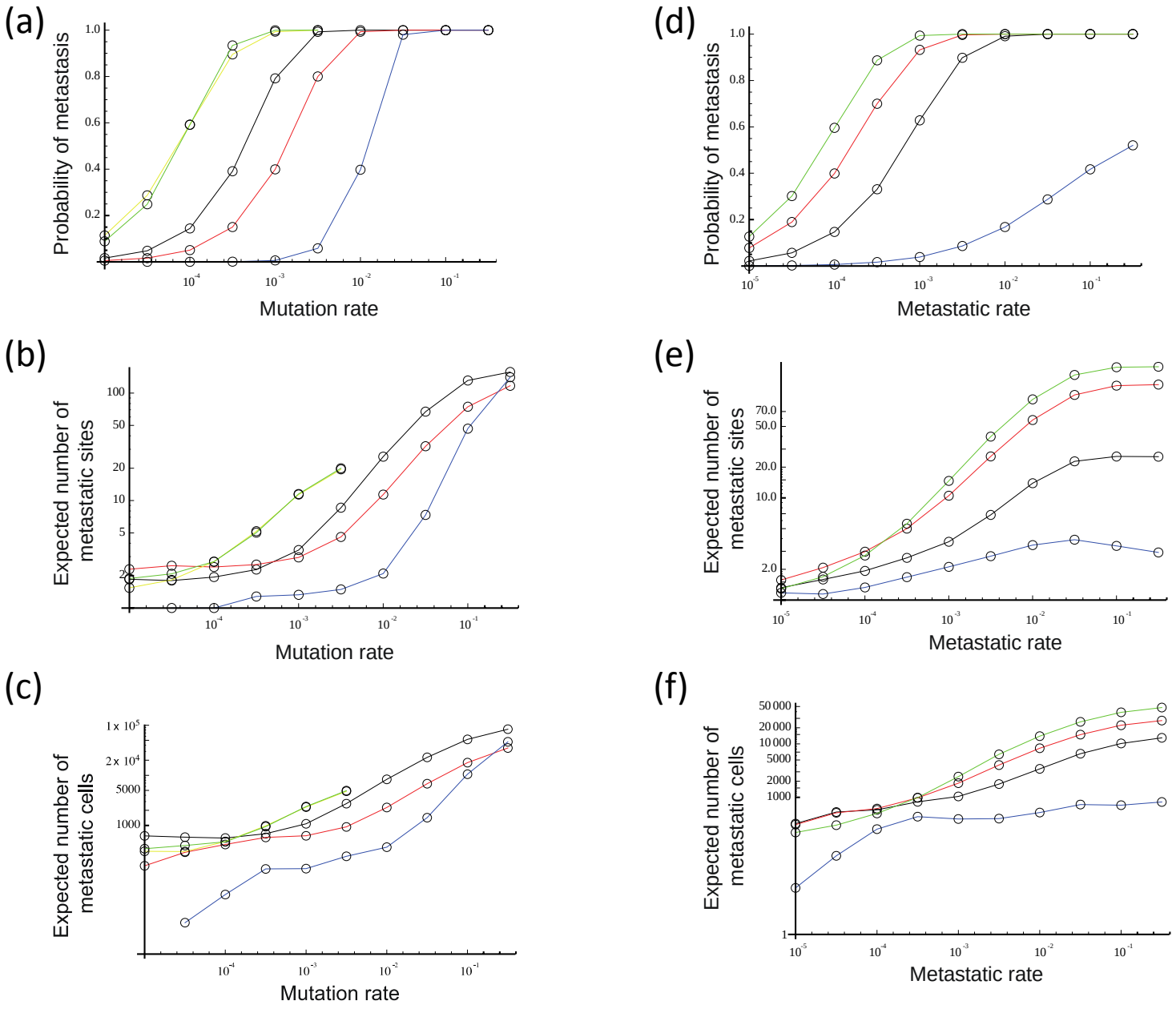
(a)
Probability of metastasis
Mutation rate
(d)
Probability of metastasis
Metastatic rate
(b)
Expected number of metastatic sites
Mutation rate
(e)
Expected number of metastatic sites
Metastatic rate
(c)
Expected number of metastatic cells
Mutation rate
(f)
Expected number of metastatic cells
Metastatic rate

(a)

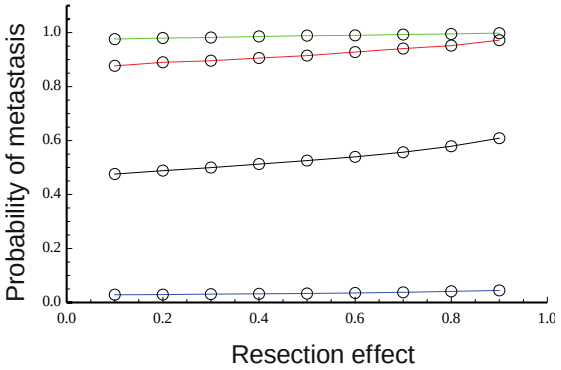
Probability of metastasis
Resection effect

(b)

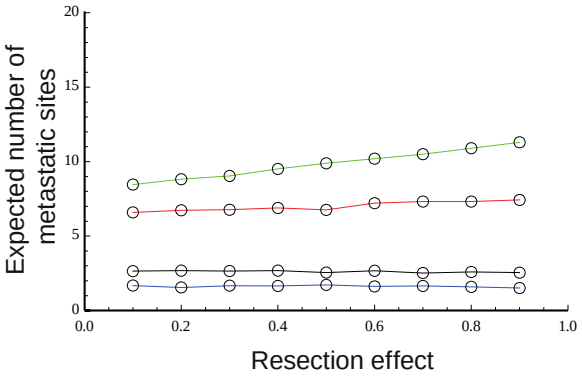
Expected number of metastatic sites
Resection effect

(c)

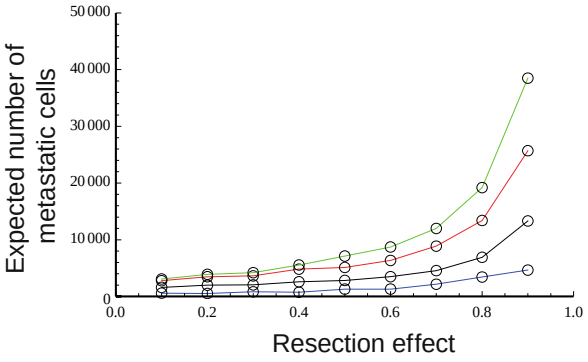
Expected number of metastatic cells
Resection effect

(d)

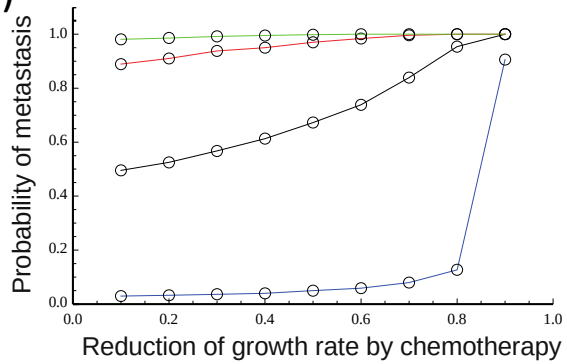
Probability of metastasis
Reduction of growth rate by chemotherapy

(e)

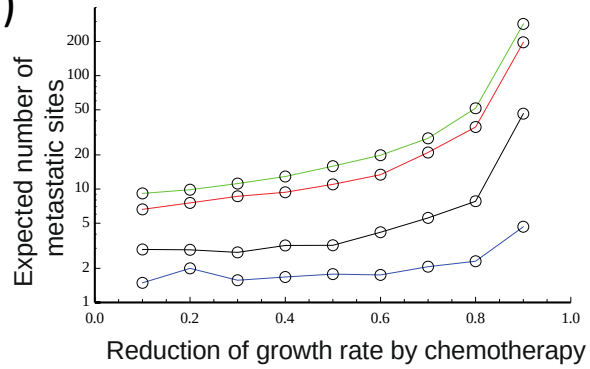
Expected number of metastatic sites
Reduction of growth rate by chemotherapy

(f)

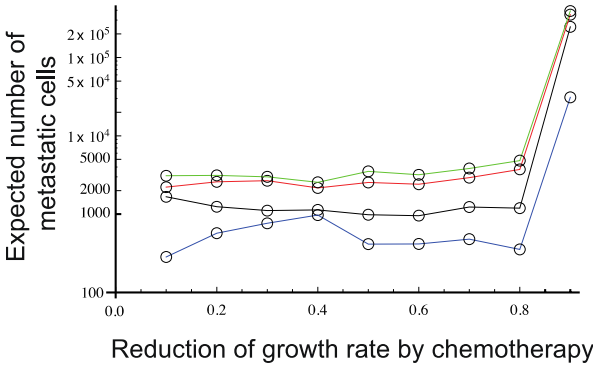
Expected number of metastatic cells
Reduction of growth rate by chemotherapy